Journal of Power Sources 196 (2011) 2422–2426

Contents lists available at ScienceDirect

Journal of Power Sources

journal homepage: www.elsevier.com/locate/jpowsour

Short communication

Electrophoretic deposition of Pt nanoparticles on plastic substrates as counter electrode for flexible dye-sensitized solar cells

Xiong Yin, Zhaosheng Xue, Bin Liu*

Department of Chemical and Biomolecular Engineering, National University of Singapore, Singapore 117576, Singapore

ARTICLE INFO

Article history:
Received 30 June 2010
Received in revised form 3 September 2010
Accepted 14 September 2010
Available online 29 September 2010

Keywords:
Electrophoretic deposition
Low-temperature fabrication
Flexible counter electrode
Dye-sensitized solar cell
Electrochemical impedance spectra
Rear-side illumination

ABSTRACT

The low-temperature fabrication of a counter electrode (CE) with low cost and high catalytic activity is one of the key steps for the practical realization of flexible dye-sensitized solar cells (DSSCs). Electrophoretic deposition is found to be an efficient method for room-temperature deposition of platinum nanoparticles on plastic substrates with low cost. The plastic CEs show increased catalytic activity and reduced transmittance when the deposited time is increased from 0 to 8 min. Under optimized conditions, flexible DSSCs based on electrophoretic deposition plastic Pt CEs and nanocrystalline TiO_2 photoanodes on Ti foil reach an energy-conversion efficiency (η) of 5.8% (under a rear-side illumination of AM 1.5 100 mW cm^{-2}), which is better than that for a device (η = 5.3%) fabricated under the same conditions with a sputtered Pt CE.

1. Introduction

Dye-sensitized solar cells (DSSCs) have been considered as potential candidates for next-generation solar cells due to the use of low-cost materials and facile fabrication methods [1–3]. A typical DSSC is comprised of a dye-sensitized semiconductor photoanode, an electrolyte-containing redox couple and a counter electrode (CE) [1]. The function of the CE is to collect electrons from the external circuit and catalyze the reduction of the redox couple [3]. To date, several materials have been used as CEs, such as platinum [3–6], carbon [7,8], conductive polymers [9–11], TiN [12], and CoS [13]. Among these materials, devices with a Pt CE have the highest efficiency of over 11% (under AM 1.5, 100 mW cm^{-2}) [3], due to its excellent electrocatalytic activity toward triiodide reduction. The Pt-based CEs are generally prepared by means of a thermal decomposition method of a Pt precursor, and display high catalytic performance with good mechanical stability. This method, however, requires a high temperature of up to 390 °C [3], which is not suitable for plastic substrates, such as polyethylene terephthalate (PET) and polyethylene naphthalate (PEN).

To fabricate flexible DSSCs, one of the key processes is the preparation of plastic CEs at low temperature with low cost [14]. So far, the most popular plastic Pt CEs have been prepared through sputtering [7] or electrochemical deposition [2]. Sputtering produces platinized electrode with high performance, but requires an ultrahigh vacuum environment and wastes source materials during deposition [5]. For the electrochemical method, platinum is deposited on the substrate surface by the reduction of a Pt (IV) salt solution under an electric field [14]. Although several DSSCs have been fabricated using Pt CEs prepared from electrochemical deposition [2], it was reported that these Pt CEs have low catalytic activity due to the inhomogeneity and poor crystallinity of the obtained Pt film [10]. Plastic CEs have also been prepared by pressing Pt-enriched Sb:SnO_2 powder on a ITO-PET substrate at room temperature [15]. This kind of CE is not, however, suitable for rear-side illumination model (lighting from CE, shown in Fig. 1) flexible DSSCs due to the opaque powder layer of CEs [16,17]. The advantages of such DSSCs based on metal foil substrates and plastic CEs are as follows: (i) no need for transparent conductive oxide; (ii) low sheet resistance; and (iii) a Ti substrate is able to endure high-temperature processing [14,16]. Considering rear-side illumination is essential for this type of flexible DSSC, it is highly desirable to develop convenient low-temperature processes for the fabrication of plastic Pt CEs with high transparency and high catalytic activity [17].

In this study, it is found that electrophoretic deposition (EPD) can be used to fabricate a Pt CE on a plastic substrate from platinum colloids at room temperature. The effects of Pt deposition conditions on the catalytic activity of CE to triiodide reduction and on the performance of DSSCs are investigated. Flexible DSSCs are fabricated with an EPD Pt CE and a nanocrystalline TiO_2 photoanode on Ti foil to show an energy-

* Corresponding author. Tel.: +65 6516 8049; fax: +65 6779 1936.
E-mail address: cheliub@nus.edu.sg (B. Liu).

0378-7753/$ – see front matter © 2010 Elsevier B.V. All rights reserved.
doi:10.1016/j.jpowsour.2010.09.047

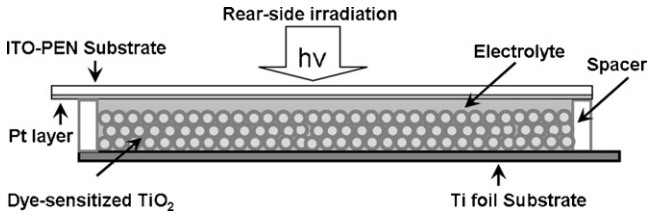

Fig. 1. Rear-side illumination model of flexible DSSCs.

conversion efficiency of 5.8% under rear-side illumination of AM 1.5 100 mW cm^{-2}.

2. Experimental

2.1. Preparation of platinum counter electrode via EPD

A platinum colloid was prepared according to the literature with minor modifications [18]: 50 mL of 0.5 mol L^{-1} NaOH (Aldrich) glycol solution (Aldrich) was added to a glycol solution of H_2PtCl_6 (0.0193 mol L^{-1}, 50 mL, Aldrich). The mixed solution was stirred at room temperature for 30 min and then heated at 120 °C for 6 h under an argon atmosphere. A dark-brown platinum nanoparticle solution was obtained after cooling to room temperature. For the electrophoretic deposition experiment, a pair of plastic ITO-PEN substrates (15 ohm □$^{-1}$, Kintec) was vertically immersed in the platinum colloid and then a 1.6 V cm^{-1} d.c. field was applied. The deposition time was set at 0.5, 1, 2, 4, 6 and 8 min, respectively. The platinum deposited electrode was rinsed with deionized water and ethanol, respectively. The electrode was heated at 60 °C for 30 min to remove water and ethanol to yield an EPD Pt CE. For comparison, flexible Pt CEs were also prepared by sputtering Pt on ITO-PEN substrates using an Auto Fine Coater (JEOL JFC-1600).

2.2. Fabrication of DSSCs

N719-sensitized TiO_2 photoanodes with a thickness of 15 μm on Ti foil (Aldrich, 0.25 mm) were prepared by the doctor-blade method according to the literature [2]. The electrolyte was a solution of 0.6 M 1-methyl-3-buytlimidazolium idode, 0.03 M I_2, 0.1 M guanidinium thiocyanate, and 0.5 M 4-tert-butylpyridine in a mixed solvent of acetonitrile and valeronitrile (v/v, 0.85/0.15). DSSCs were fabricated by sandwiching a TiO_2 photoanode and a counter electrode with electrolyte in a 25 μm thick spacer made by a thermobonding film (Surlyn, Dupont). The active area of the cells was 0.158 cm^2.

2.3. Characterization

X-ray photoelectron spectroscopy (XPS) of an EPD Pt/ITO-PEN electrode was obtained with a Kratos Axis Ultra instrument (Shimadzu). A transmission electron microscope (TEM) (JEOL JEM-2010F) was employed to investigate the morphology and distribution of the platinum nanoparticles. Electrochemical impedance spectroscopy (EIS) was carried out with an AutoLAB PGSTAT 320N Potentiostat (ECO Chemie B.V.). The EIS for two identical platinized flexible electrodes [19] was conducted with zero bias potential in the frequency range between 10^5 Hz and 0.05 Hz with a 5 mV a.c. amplitude. The EIS for a DSSC was recorded over a frequency range between 0.01 Hz and 10^6 Hz under a rear-side illumination of 100 mW cm^{-2}. The applied bias voltage and a.c. amplitude were set at the open-circuit voltage of the DSSC and 10 mV, respectively. The EIS spectra were analyzed using an equivalent circuit model. Transmittance of flexible CEs was measured using a UV–Vis spectrophotometer (Shimadzu, UV-1700). The photovoltaic parameters of DSSCs were performed by an AutoLAB PGSTAT 320N Potentiostat with simulated light (AM 1.5 100 mW cm^{-2}, San Ei, Japan).

3. Results and discussion

3.1. Characterization of Pt electrode prepared via EPD

The surface composition of an EPD Pt/ITO-PEN electrode was investigated by XPS analysis. As shown in Fig. 2a, peaks for Pt4f and Pt4d electrons appear in the spectra, indicating that Pt particles have been successfully deposited on a plastic substrate *via* EPD. The magnified view of Pt4f is shown in Fig. 2b. The binding energies of $Pt4f_{7/2}$ and $Pt4f_{5/2}$ electrons are 71.1 and 74.4 eV, respectively, which indicate that Pt on the ITO-PEN surface has zero valence [18]. A representative TEM image of Pt nanoparticles on an electrode *via*

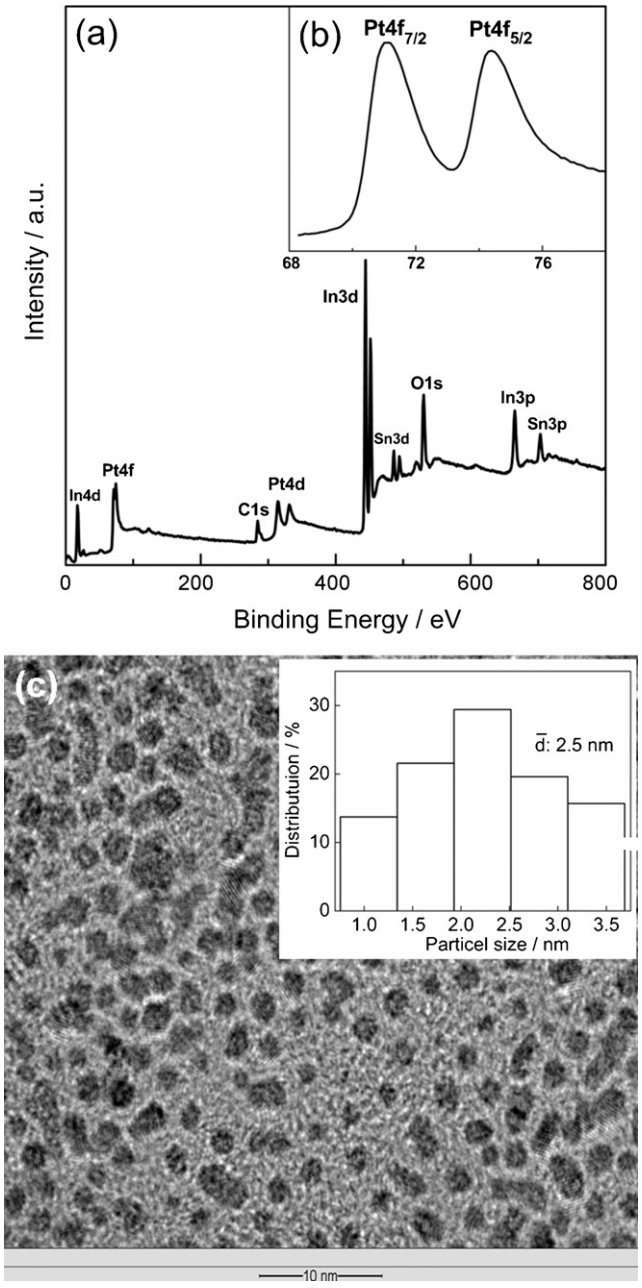

Fig. 2. (a) XPS spectra of EPD Pt/ITO-PEN electrode; (b) magnified view of Pt4f XPS spectra; and (c) TEM image of Pt nanoparticles prepared *via* EPD for 6 min. Inset shows distribution of Pt nanoparticles.

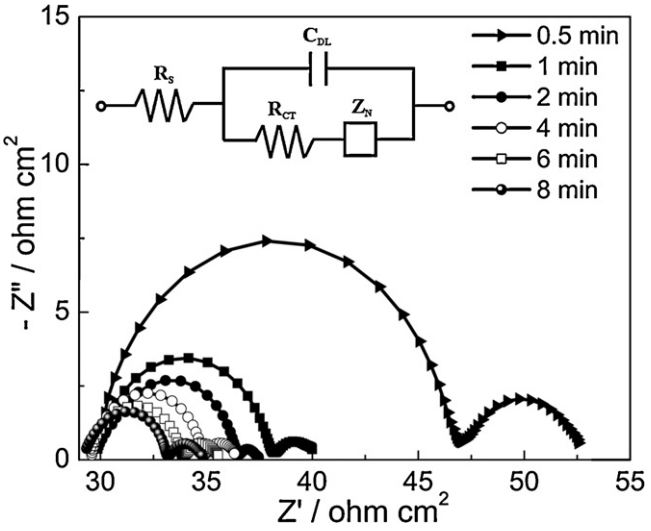

Fig. 3. Nyquist plots of thin layer electrochemical cell consisting of two identical EPD Pt/ITO-PEN electrodes with different deposition times. Inset shows equivalent circuit.

Table 1
Impedance parameters of CEs prepared with different deposition times estimated from Nyquist plots in Fig. 3.

Deposition time (min)	R_S (ohm cm^2)	R_{CT} (ohm cm^2)
0.5	29.97	8.51
1	29.87	4.03
2	29.82	3.16
4	29.60	2.61
6	29.50	2.16
8	29.35	1.96

EPD for 6 min is shown in Fig. 2c. The diameter of Pt particles is in the range of 1–4 nm with an average particle size of 2.5 nm.

3.2. Electrocatalytic activity of EPD Pt counter electrode

The electrocatalytic activity of plastic Pt CEs was evaluated using EIS by measuring the charge-transfer resistance (R_{CT}), which is an index of the catalytic performance of Pt electrodes. Nyquist plots of EPD Pt electrodes deposited with different deposition times are shown in Fig. 3. The semicircle in the high frequency corresponds to the R_{CT} of a Pt electrode|electrolyte interface, while the semicircle at low frequency represents the Nernst diffusion impedance (Z_N) of the I^-/I_3^- redox species. The intercept of the real axis at high frequency is the ohmic series resistance (R_S), corresponding to the overall series resistance of the device [19]. The equivalent circuit is shown in the inset of Fig. 3. These devices show a similar value of R_S of about 30 ohm cm^2. The R_{CT} value was calculated as half of the value obtained from the equivalent circuit, and the values of R_S and R_{CT} are listed in Table 1. As shown in Fig. 3, the circle at high frequency becomes smaller with an increase in the deposition time from 0.5 to 6 min. When the deposition time is above 6 min, there is no significant change in R_{CT}. The R_{CT} values are 8.52, 4.03, 3.16, 2.61, 2.16 and 1.96 ohm cm^2 for a deposition time of 0.5, 1, 2, 4, 6 and 8 min, respectively. The decrease in R_{CT} value is related to acceleration of triiodide reduction by the Pt layer, and lower R_{CT} value indicates higher catalytic activity of CEs. Since a R_{CT} value of less than 10 ohm cm^2 has been generally acceptable for DSSCs [7,14], these results clearly indicate that the flexible Pt electrodes prepared through EPD at low temperature can be applied as CEs in DSSCs.

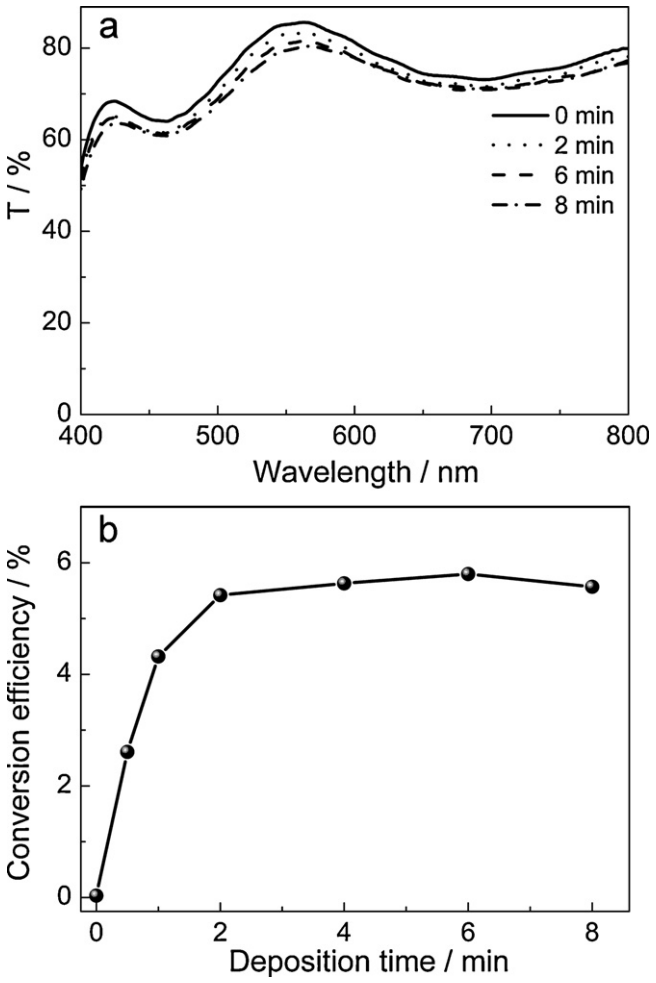

Fig. 4. (a) Light transmittance of CEs prepared with different deposition times and (b) change in energy conversion efficiency of flexible DSSCs with deposition time of CEs.

3.3. Photovoltaic performance of DSSCs

As shown in Fig. 1, since rear-side irradiation is required for flexible DSSCs with a nanocrystalline TiO_2 thin film on Ti foil as the photoanode, the transparency of plastic CEs is an important determinant of the device performance [16,17]. The light transmittance of CEs prepared with different deposition times is given in Fig. 4a. The CE transparency decreases with increased deposition time from 0 to 8 min, but the transmittance of the obtained CEs is over 70% within the range of 500–800 nm, and this indicates that EPD CEs are good for rear-side illumination. When these CEs are used to fabricate DSSCs under the same conditions, the changes in device energy conversion efficiency (under rear-side illumination, 100 mW cm^{-2} AM 1.5) with deposition time are presented in Fig. 4b. There is a significant increase in energy-conversion efficiency (η) from 0.03% with a fill factor (FF) of 0.04% to η = 5.42% and FF = 0.53 when the deposition time is increased from 0 to 2 min. The conversion efficiency increases slightly to 5.80% with a FF of 0.65 when the deposition time is extended to 6 min. Further increasing the deposition time to 8 min leads to a reduced device efficiency with a η of 5.55% and a FF of 0.65.

The effect of Pt CEs with different deposition times on the photovoltaic characteristics of the DSSCs can be investigated with the aid of EIS conducted under light illumination. The EIS spectra for DSSCs fabricated with Pt CEs prepared at different deposition times are shown in Fig. 5, and the equivalent circuit is given in the

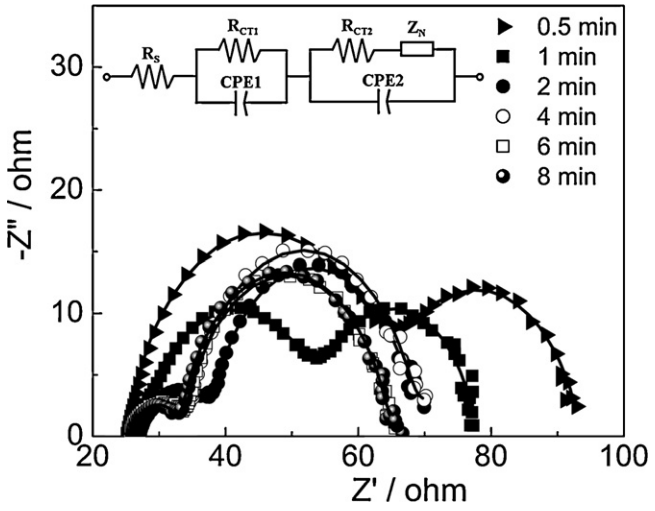

Fig. 5. Electrochemical impedance spectra of DSSCs with different deposition times of CEs, measured under rear-side irradiation of 100 mW cm^{-2} AM 1.5 at open-circuit voltage. Solid lines show fitted results, and inset shows equivalent circuit.

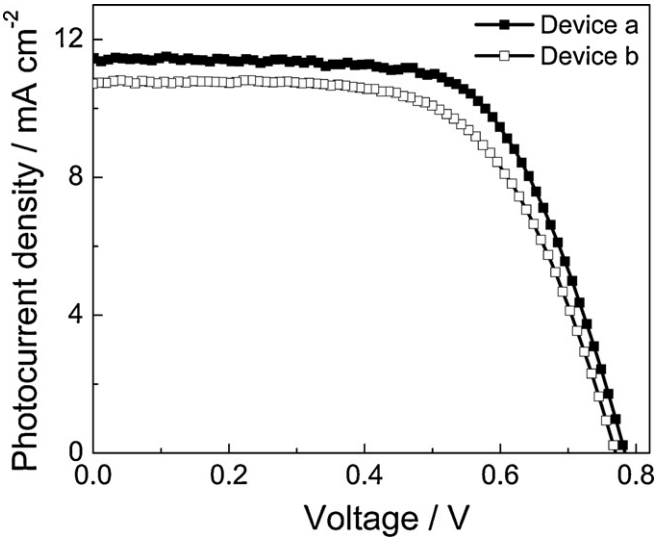

Fig. 6. Photovoltaic characteristics of flexible DSSCs with plastic EPD Pt CE (Device a) and plastic sputtered Pt CE (Device b), measured under rear-side irradiation of 100 mW cm^{-2} AM 1.5.

inset [16,20]. Generally, three characteristics semicircles can be obtained from EIS spectra in the frequency range between 10^6 Hz and 0.01 Hz. The high-frequency arc is ascribed to the charge-transfer resistance at the interface of the counter electrode and the electrolyte (R_{CT1}). The middle frequency arc is related to charge transfer and recombination at the TiO_2–dye–electrolyte interfaces (R_{CT2}). The low-frequency arc is attributed mainly to Nernst diffusion of I^-/I_3^- within the electrolyte (Z_N) [16,20,21]. As shown in Fig. 5, two main semicircles are observed and the third semicircle of Z_N is not obvious and overlapped by R_{CT2} because of the low viscosity of the present electrolyte [16]. The fitted values of R_{CT1} and R_{CT2} are summarized in Table 2. The R_{CT1} rapidly decreases with increase in deposition time from 0.5 to 2 min, indicating enhancement of the catalytic ability of the Pt layers. The decrease in R_{CT1} can result in a higher FF and conversion efficiency [20,21]. The R_{CT1} stays almost unchanged with further deposition. When the deposition time is over 4 min, the R_{CT2} shows a similar value for different deposition times. In addition, the value of R_{CT2} is about 4 times larger than that of R_{CT1}, and the R_{CT2} is the main factor in determining the photovoltaic characteristics of DSSCs. The change in conversion efficiency is related to a change in the total resistance (R_{TOTAL}), which determines the photovoltaic performance of the DSSC [20,21]. In a DSSC, the total resistance can be expressed as:

$$R_{TOTAL} = R_S + R_{CT1} + R_{CT2} + Z_N \quad (1)$$

where R_S is the substrate resistance [21]. The Z_N is overlapped by R_{CT2}, so that Eq. (1) can be reduced to:

$$R_{TOTAL} = R_{TCO} + R_{CT1} + R_{CT2} \quad (2)$$

The resistance R_S can be taken as constant for devices fabricated under the same conditions. The decrease in the sum of R_{CT1} and R_{CT2} with increased deposition time thus leads to a reduction in R_{TOTAL}, which helps to improve the FF and conversion efficiency. The results are consistent with the data obtained from the photovoltaic characteristics. The energy-conversion efficiency shows a peak value of 5.8% at the deposition time of 6 min for the fabricated flexible DSSCs.

Table 2
Electrochemical impedance parameters of DSSCs with different deposition times of CEs, measured under rear-side irradiation of 100 mW cm^{-2} AM 1.5.

Deposition time (min)	R_{CT1} (ohm)	R_{CT2} (ohm)	$R_{CT1}+R_{CT2}$ (ohm)
0.5	29.01	29.16	58.17
1	21.58	28.52	50.10
2	12.61	29.78	42.39
4	7.98	33.03	41.01
6	7.83	30.00	37.83
8	7.74	31.73	39.47

To compare the performance of CE prepared from EPD with that from sputtering, CEs were also prepared by sputtering Pt on ITO-PEN to reach the same transparency (72% at 500 nm) as that for an EPD CE for a Pt deposition for 6 min. The corresponding devices were fabricated under the same conditions, and the photovoltaic characteristics are shown in Fig. 6. The DSSCs (Device b) with sputtered Pt CE exhibit an open-circuit voltage (V_{oc}) of 0.77 V, a short-circuit current density (J_{sc}) of 10.71 mA cm^{-2}, and a FF of 0.64, which yield an energy-conversion efficiency of 5.3%. This is slightly lower than that based on EPD CE (Device a, 5.8%, 0.78 V, 11.44 mA cm^{-2}, 0.65). These results demonstrate that EPD CEs have shown a similar catalytic activity for triiodide as that of CEs prepared by sputtering, and EPD is an effective low-cost method for CE fabrication at low temperature with high catalytic activity for flexible DSSCs.

4. Conclusions

A low-cost, low-temperature fabrication method for Pt CE on plastic substrates *via* electrophoretic deposition has been developed. The optimized EPD Pt CEs display high catalytic activity, which is comparable to that of CEs obtained through sputtering and are ideal for flexible DSSC fabrication. An energy-conversion efficiency of 5.8% is achieved for flexible DSSCs with EPD Pt/ITO-PEN CE, and TiO_2 photoanode on Ti foil. The low-temperature fabrication procedure also eliminates the need for a high vacuum and a large amount of source material and is thus ideal for flexible DSSCs.

Acknowledgements

The authors are grateful to the National Research Foundation of Singapore (NRF-279-000-276-272) for financial support. X. Yin thanks W. Zhang and X. Z. Liu for valuable discussions.

References

[1] B. O'Regan, M. Grätzel, Nature 353 (1991) 737–740.
[2] S. Ito, N.-L.C. Ha, G. Rothenberger, P. Liska, P. Comte, S.M. Zakeeruddin, P. Pechy, M.K. Nazeeruddin, M. Grätzel, Chem. Commun. 38 (2006) 4004–4006.
[3] T.N. Murakami, M. Grätzel, Inorg. Chim. Acta 361 (2008) 572–580.
[4] G.Q. Wang, R.F. Lin, Y. Lin, X.P. Li, X.W. Zhou, X.R. Xiao, Electrochim. Acta 50 (2005) 5546–5552.
[5] P. Hasin, M.A. Alpuche-Aviles, Y.G. Li, Y.Y. Wu, J. Phys. Chem. C 113 (2009) 7456–7560.
[6] F.S. Cai, J. Liang, Z.L. Tao, J. Chen, R.S. Xu, J. Power Sources 177 (2008) 631–639.
[7] K.X. Li, Y.H. Luo, Z.X. Yu, M.H. Deng, D.M. Li, Q.B. Meng, Electrochem. Commun. 11 (2009) 1346–1349.
[8] G.Q. Wang, W. Xing, S.P. Zhuo, J. Power Sources 194 (2009) 568–573.
[9] W.J. Hong, Y.X. Xu, G.W. Lu, C. Li, G.Q. Shi, Electrochem. Commun. 10 (2008) 1555–1558.
[10] J.H. Wu, Q.H. Li, L.Q. Fan, Z. Lan, P.J. Li, J.M. Lin, S.C. Hao, J. Power Sources 181 (2008) 172–176.
[11] K.-M. Lee, P.-Y. Chen, C.-Y. Hsu, J.-H. Huang, W.-H. Ho, H.-C. Chen, K.-C. Ho, J. Power Sources 188 (2009) 313–318.
[12] Q.W. Jiang, G.R. Li, X.P. Xiao, Chem. Commun. 41 (2009) 6720–6722.
[13] M.K. Wang, A.M. Anghel, B. Marsan, N.-L.C. Ha, N. Pootrakulchote, S.M. Zakeeruddin, M. Grätzel, J. Am. Chem. Soc. 131 (2009) 15976–15977.
[14] M. Toivola, J. Halme, K. Miettunen, K. Aitola, P.D. Lund, Int. J. Energy Res. 33 (2009) 1145–1160.
[15] H. Lindstrolm, A. Holmberg, E. Magnusson, S.-E. Lindquist, L. Malmqvist, A. Hagfeldt, Nano Lett. 1 (2001) 97–100.
[16] L.-Y. Lin, C.-P. Lee, R. Vittal, K.-C. Ho, J. Power Sources 195 (2010) 4344–4349.
[17] L.L. Chen, W.W. Tan, J.B. Zhang, X.W. Zhou, X.L. Zhang, Y. Lin, Electrochim. Acta 55 (2010) 3721–3726.
[18] Y. Wang, J.W. Ren, K. Deng, L.L. Gui, Y.Q. Tang, Chem. Mater. 12 (2000) 1622–1627.
[19] X. Yin, W.W. Tan, J.B. Zhang, Y.X. Weng, X.R. Xiao, X.W. Zhou, X.P. Li, Y. Lin, Colloids Surf., A 326 (2008) 42–47.
[20] L.Y. Han, N. Koide, Y. Chiba, A. Islam, R. Komiya, N. Fukui, R. Yamanaka, Appl. Phys. Lett. 86 (2005) 213105–213107.
[21] F. Fabregat-Santiago, J. Bisquert, E. Palomares, L. Otero, D. Kuang, S.M. Zakeeruddin, M. Gratzel, J. Phys. Chem. C 111 (2007) 6550–6560.